Original scientific paper

Informacije MIDEM
Journal of Microelectronics,
Electronic Components and Materials
Vol. 45, No. 3 (2015), 204 – 215

Grid-Tied Smart Inverter Safety Functionality: Fast Power Quality Event Detection

Isabel M. Moreno-Garcia, Antonio Moreno-Munoz, Aurora Gil-de-Castro, Rafael Real-Calvo, Emilio J. Palacios-Garcia, Miguel J. González-Redondo

Department of Computer Architecture, Electronics and Electronic Technology, University of Cordoba, C. Rabanales, Ed. Leonardo Da Vinci, Cordoba, Spain

Abstract: This paper addresses the fast detection of electric signal disturbance for advanced smart inverter functionality within the framework of large scale grid integration of renewable energy sources. A statistical-based technique under the fault detection and isolation (FDI) paradigm is proposed for fast detection in power systems. The aim is to improve the performance of interconnection systems and the electricity grid's energy efficiency. The new method developed is based on the CUmulative SUM (CUSUM) algorithm and is applied to a wide set of power quality events to analyse its performance. The results show that the method generates residuals that are robust to noise and accurately estimates the time locations of underlying transitions in the power system. The main advantage of the proposed technique is its early event detection, with respect to other traditional methods, because it performs sample-by-sample evaluations. Moreover, the proposed technique does not require much computational effort, which means that the presented detection method is suitable for integration into the multifunction relay protection subsystems available in novel smart inverters.

Keywords: Change detection algorithms; event detection; power quality; power system protection; real-time system

Varnostna značilnost pametnega omrežnega razsmernika: Hitra detekcija dogodka kvalitete moči

Izvleček: Članek naslavlja hitro detekcijo moten električnega signala pri naprednih pametnih razsmernikih v okvirju široke omrežne integracije obnovljivih virov energije. Za hitro detekcijo je predlagana statistična metoda odkrivanja napak in njihovih izolacij (FDI). Cilj raziskave je izboljšanje povezav in učinkovitost prenosa električne energije. Nova metoda temelji na kumulativnem seštevalnem algoritmu (CUSUM), ki je z namenom analize učinkovitosti apliciran na širok set dogodkov kvalitete moči. Rezultati nakazujejo, da metoda generira ostanke, ki so neobčutljivi na šum in natančno ocenjujejo časovno lokacijo osnovnih prenosov v sistemu. Največja prednost predlagane tehnike, v primerjavi z obstoječimi, je hitra detekcija dogodka na osnovi medvzorčnih ocen. Nadalje, nova tehnika ne zahteva velike računske moči, zaradi česar je primerna za integracijo v večopravilne stikalne zaščitne sisteme razsmernika.

Ključne besede: algoritem detekcije sprememb; detekcija dogodkov; kvaliteta moči; zaščita močnostnega sistema; sistem v realnem času

* *Corresponding Author's e-mail: p92mogai@uco.es*

1 Introduction

Nowadays, energy is a vital means of achieving social development. Nevertheless, energy production is a source of significant environmental impact, and the improper use of increasing amounts of energy is one of the factors involved in major potential environmental degradation. The transition to a more sustainable societal model is perhaps the most important challenge faced today. The increasing pressure on natural resources due to the introduction of millions of new consumers to markets, economic dependency on energy sources located outside of our territories, and climate change, as a consequence of increased global warming in recent decades, are only some of the issues that must be addressed to prevent reductions in levels of well-being.

© MIDEM Society

One method of avoiding this unbalance is for industrialised countries to reach environmental sustainability by decreasing their energy intensity, reducing their consumption of fossil fuels, diminishing greenhouse gas emissions and increasing the security of their energy supply [1]. In this context, a long-term commitment to renewable energy sources (RES) seems to be the only adequate answer to all of these issues. An example can be seen in the recent solar boom of 2010-12 and its integration into electrical systems in different countries. However, the growing penetration of solar generation raises several economic, regulatory and technical questions, some of which are closely related to power quality (PQ) [2]. Moreover, the growing coexistence of both conventional and distributed generation in the same electrical system is causing a reconsideration of the traditional power system towards the smart grid. This approach will require the global integration of large numbers of independent and autonomous systems from different stakeholders. Due to the market trend towards diversifying distributed energy resources (DERs), large infrastructure systems, such as the electric power grid, may be viewed as complex systems-of-systems. This will pose new challenges for the integration of these intelligent sub-systems, so they can participate collectively and in a timely manner. This radical shift from the traditional centralised philosophy will require the implementation of real-time information in the whole electrical system.

DERs not only include generation units but also aggregated flexible resources like storage for electrical and thermal energy and/or flexible loads. Thus, DER systems that generate AC output, often with variable frequencies, such as wind, microturbine or flywheel storage, need AC-DC conversion. For DC output systems like PV, fuel cells and batteries, a DC-DC conversion is typically needed to change the DC voltage level. Accordingly, MW-scale power electronics converters are essential components in new DER plants. Due to advancements of technology, the costs of power electronics have decreased significantly, sizes have also become smaller and performance has improved. Up to now, most DERs only produce power; they do not contribute to the ancillary services required to control the power system and ensure stable operation. However, the main inconveniences of DERs include their inherent variability and uncertainty.

Part of the solution to moderating the impact of DERs on the grid lies in the DER units themselves, particularly in the interconnection equipment, such as inverters, that connects DERs to the electric power system. Driven by Germany's 2011 LV-MV Directives [3], inverters can contain smart features such as reactive power control to aid with grid integration. By the end of 2015, over 50% of inverters can carry these functions. This percentage could increase through disruptive energy-storage innovations being incorporated into the inverter [4].

Thus, there is a growing need for a high-performance embedded system that supports both existing functionalities and future operational requirements. Standards like IEC 61727 [5], IEEE 1547 [6] and VDE 0126-1-1 [7] establish criteria and requirements for the interconnection of DERs with electric power systems. The requirements shall be met at the point of common coupling (PCC). Although the devices used to meet these requirements can be located elsewhere, the current trend is to include it within the inverter itself [8,9]. Recently, we have presented the complete characteristics of a smart inverter for distributed energy resources (SIDER), and some possible new active functions can still be developed [10,11]. In the smart grid, SIDER can contribute to the reliability and stability of the entire power-supply infrastructure. It must respond to PQ events and fault conditions within the sub-cycle range by incorporating extremely fast response times. What is more, due to market expectations, self-diagnosis and self-healing functionalities must play a fundamental role in achieving the high PQ demanded, as well as subsequent trust in the smart grid paradigm.

The rest of this paper is organised as follows. An overview of the methods proposed for detecting of PQ disturbances is presented in Section 2. In Section 3, we propose a statistically based detection method with an FDI approach. Section 4 studies the performance of the method detecting different PQ disturbances. Finally, the conclusions are given in Section 5.

2 Detection of power quality events

The automated power quality analysis entails the following stages: the detection, segmentation and characterization of the power quality event. This information is useful to determine its cause and to establish limits of responsibilities between a network operator and final customer. An extensive and updated classification of different techniques available can be found in [12]; unfortunately, an analysis of their suitability for each of the above mentioned stages has not been clearly established. These stages can be preceded by a pre-processing stage of signal de-noising and normalisation. We have addressed the second and third stages thoroughly in prior works [13–18]. Thus, this paper focuses on the experimental research effort toward fast detection of electric signal disturbance within the framework of advanced smart inverter requirements.

Nowadays, well-known signal processing methods have been applied to detect PQ disturbances with satisfactory results. Evaluating electrical system disturbances involves studying voltage and current deviations from the ideal waveform. In general, these deviations can be classified into two groups under the PQ paradigm: variations and events [19]. The former (eg, harmonics, overvoltages, unbalances, etc.) are generally regarded as small and gradual deviations from the voltage/current sine wave, characterised as steady-state phenomena; the latter produce sudden, large deviations of the waveform, are characterised as non-stationary random phenomena, and are usually caused by incidents involving the electrical system's operation conditions. According to [20], the event detection methods can be grouped into time-dependent waveform feature [21], signal transformation [22] and parametric models [20]. Many studies have analysed the advantages and disadvantages of these methods. In particular, [23], shows the statistical performance of various detectors of a signal affected by a dip, using methods based on root mean square (RMS), Kalman filter, wavelet, peak voltage, missing voltage and generalized likelihood ratio test (GLRT). However, despite the wide range of PQ event parameters (frequencies, magnitudes, and durations), it is difficult to find a single method that is suitable for detecting of all types of them. For example, the commonly used wavelet transform is suitable for detecting of transients but fails for short- and long-duration variations (such as sags and swells, particularly those with a nonrectangular shapes) [24]. The situation is similar for HOS; the behavioural differences in frequency between the transients and sag (or swell) demands, which the sliding window used to extract HOS features, were completely different in both cases. For the transients, after a high-pass filter, the width of the window may be less than one cycle; for the last events, which are roughly of the same frequency as the "healthy" signal (ideal power-line sine wave), the window must contain a cycle of the 50-Hz sine wave [25]. Thus, in this paper, to unify the statistical treatment of all PQ events, it will be necessary to choose a new variable that exclusively distils the information of the perturbation from the waveform, without any losses (a descriptor).

Moreover, disturbance detection is a critical task and an effective protection requirement that is needed to successfully control the interconnection of a DG system to the grid. It must be performed on-line and in strict real-time, with the less number of false detection and accomplishing the temporary response specifications suitable for monitoring parameters and planned protective actions. Fig. 1 shows a comparison of the main standards in PQ applications and protection, referring to the response times needed to disconnect the equipment of the DG system's equipment when the voltage exceeds the allowable operating ranges.

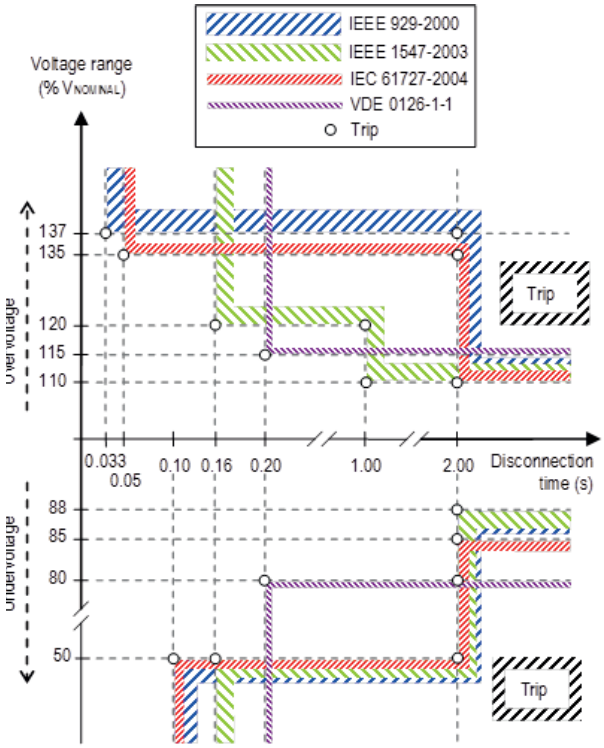

Figure 1: Comparison of responses to abnormal voltage according to different standards.

As shown in Fig. 1, IEEE 929 [26] and IEC 61727 [5] are very similar with respect to operating ranges and disconnection times. In these standards, being outside the normal range of operation is necessary to disconnect the equipment in < 2 s. One can see that at a relatively large distance from the percentage of nominal voltage, the trip points require low disconnection times (≤ 0.10 s). IEEE 1547 [6] aims for such high percentages of rated voltage to not be achieved, seeking a compromise solution to the overvoltages, so that disconnection times can be increased. Finally, the VDE 0126-1-1 [7] standard seeks to provide a compromise solution and greater simplicity in controlling the device with only two trip points for overvoltages and undervoltages, respectively.

Thus, to prevent failures of high relevance to the power system, the protection devices integrated with the grid must be able to detect disturbances in early stages. We are definitely dealing with a problem of change point detection within the FDI domain, in response to the specific fault. A thorough survey can be found in [27]. The problem of change detection has remained an area of strong interest in recent years, as well as the study of parametric statistical tools for detecting abrupt changes in discrete time signals and dynamic systems [28,29]. According to the model-based filtering

introduced in [29], and bearing in mind that most of the detection methods use a detection parameter (DP) joint a threshold, the detection of abrupt changes in the processed signals can be conceived in three steps:

- *Residual generation:* The basic principle is that residuals from are generated signal modelling. These residuals are expected to be zero (or zero mean) under no-fault conditions. In practical situations, the residuals are corrupted by the presence of noise, unknown disturbances, and uncertainties in the system model. The aim of the method is to generate robust residuals insensitive that are to these noises and uncertainties but are sensitive to faults.
- *Detection parameter generation:* The filter residuals must be treated in order to be transformed into a distance measure (DP) that measures the deviation from the no-change hypothesis.
- *Stopping rule:* This step is based on a statistical algorithm to make decisions on whether the deviation of a DP is significant.

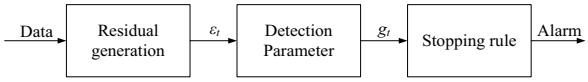

Figure 2: Block diagram of the detection method based on filtering [29].

3 The proposed detection algorithm

This work mainly focuses on a quantitative model-based approach to FDI, so that it can be used to develop more efficient and reliable equipment. The detection methods included in an intelligent electronic device (IED) allow PQ measurement and provide, protection functions and predictive tools, making the device ready to be used in the new smart grid model with the characteristics described in [30], i.e. fast registration of the events, transmission to the power network control system and smart relay protection devices [5].

In our work [31] a high-capacity IED was designed to be embedded into inverter equipment took PQ, protective relay functions and synchronisation standards into account. For a fast activation of the protection functions, the detection instant should be as close as possible to when the disturbance start. Therefore, the analysis window should be as short as possible. Thus, the requisites of the algorithm are low computational load, high accuracy and robustness. What is more, if we wanted to detect the event in real-time the challenge is to make the decision in less than a half-cycle, obviously. In prior work [31], a detection method based on a CUSUM test of Page was initially proposed. In that work, the signals used were generated by a power system with a frequency was 50 Hz, in which the IED captured every half cycle (10 ms) while operating in real-time [11]. The CUSUM algorithm was selected because it operates sample to sample, making it suitable for fast detection. This algorithm accumulates the difference between the sample mean and a target mean, and plots it cumulatively. A change in the DP gradient, either increasing or decreasing, indicates a departure from the normal circumstances of the residual values [32,33]. The acquisition process, which is executed with a high priority loop, is joined in the detection process by CUSUM, which is executed with a normal priority loop that occurs in a time below 10 ms. The preliminary results from applying the CUSUM algorithm to real-time PQ detection were sufficient but not entirely satisfactory, as will be explained below. Moreover, the method's performance was only quantified using synthetic disturbances.

Thus, this paper provides a following step and analyses the CUSUM method with real three-phase disturbances. A modification of the original algorithm proposed in [31] is needed to detect an event in a real environment with the lowest number of false detection. The new proposed technique for fast detection of three-phase events and the new methods used to generate residuals are presented here; additionally, the rules to calculate the DP and decide whether to stop are thoroughly described.

3.1 Residual generation

As mentioned above, the aim of the residual generation in our work [31] was to model the signal in order to obtain robust residuals that are insensitive to these noises and uncertainties but are sensitive to faults. To this end, the first idea suggested was a unified analysis of the three-phase power system using the Clark Transform. However, for an unbalanced event, the transformation output adds a ripple component over the DC value, which is twice the source fundamental frequency f_o. To get the DC values, a notch filter or a low-pass filter with a its cut-off frequency lower than $2*f_o$ Hz is recommended to remove the ripple component [34–36]. Unfortunately, the use of an additional filtering step causes a delay in the event detection; hence it increases the response time, which results in a delay in the overall response time.

Therefore, a new method was needed here to overcome the above mentioned deficiency. A simple method called the peak detection method [37, 38], generally used in power electronics converters [39, 40], can be used to obtain our input variable. The peak detection method offers fast response time as well which, of less than a quarter of a cycle. This method is very simple

to implement and has a low computational burden; however when it was applied in real environment, it proved very sensitive to noise. Thus, the peak detection method was rejected in the early stages of this research.

A filtering method was finally considered. In residual generation, an adaptive filter takes the measured signal and transforms it into a sequence of residuals that are similar to white noise before the change occurs. The filtering approach is used to separate the signal from the noise. For this purpose, finite impulse response (FIR) or infinite impulse response (IIR) filters can be used, as long as designed by any standard method (Butterworth, Chebyshev, etc.) [29]. In this work, a high pass Butterworth filter was used to generate the residuals.

3.2 Detection parameter algorithm

The next step is to threat the residuals through a statistical algorithm in order to detect any abrupt change in the input signal early. To this end, several approaches can be used: analysing of the mean or variance of the residuals, analysing the square of the residuals or other options based on probability ratios.

In this work, the statistical algorithm used to develop the mentioned change detector (DP) is the CUSUM method, which is based on the mean and variance of the residuals. It was selected method because it requires minimal computational effort and operates sample to sample, which it is very appropriate for fast online detection. The change detection of the CUSUM method is labelled as a change in the mean of the filtered signal. The input to the CUSUM algorithm is called distance the measure, s_t, which is set with the residuals from the filter, $s_t = \varepsilon_t$ (Fig. 2).

The CUSUM algorithm directly includes all of the information in the sample sequence by plotting the cumulative sums of any deviation of the sample values from a target value. The CUSUM method is widely used across industries for monitoring deviations in a process with respect to a target value and also for finding evidence of change in the a process's mean; in particular, it has been successfully employed in power system fault detection [29, 42–44]. The CUSUM method is easy to handle and useful for detecting the locations of change points. The combination of information from several samples makes the CUSUM algorithm a suitable method for detecting abrupt changes of PQ events in real-time. The CUSUM version used in [31] was the so-called tabular or two-sided CUSUM method [28,32]; it was designed to detect high and low changes in mean processes, as well as record the cumulative sums of the signal samples in two directions. In this paper, the DP proposed to detect disturbances is only based on the statistical estimator for detecting an increase in the mean of the residuals, which is given by Eq. (1).

$$g_t = \max\left(g_{t-1} + s_t - \left(\mu_0 + K\right), 0\right) \quad (1)$$

where the DP, which is named g_t, sums the inputs s_t from the filter. In Eq. (1), μ_0 is the ideal mean of the process control state and K is the reference value set with a value that allows for a fast fault detection, which is usually half of the difference between the value of the average target control state and the value of the average at which the process is considered out of control [32]. The constant value given by the sum of μ_0 and K has been removed to prevent false alarms. In this work, unlike the previous one [31], these parameters are configured. The μ_0 parameter has been set to the mean of the samples processed to the current time, and the K parameter was configured at 0.5 times the standard deviation of the filtered signal.

3.3 Stopping rule

The purpose of the stopping rule phase is to detect when a process is considered to be out of control. In signal processing, the aim is to give an alarm when any statistic crosses a decision interval called a threshold, H. As mentioned above, non-zero residuals are generated if there is a disturbance in the processed signal. This situation produces a change in the mean of the samples processed at the current time, so that the change detection algorithm, g_t, must indicate the variation. The main problem in statistical change detection is determining the optimal threshold value to obtain high accuracy in change detection and a low rate of false alarms.

Regarding the preliminary results obtained with synthetic signals, the DP deviations from zero were considered to be produced by changes in the pure sinusoidal shape of the signal. However, with the measured signals, false alarms were generated in many cases when the threshold H was initialised to zero. To set a threshold H that avoids false alarms, 127 measured events were filtering and analysed. Later, the CUSUM algorithm was used to obtain the DP, and the results were studied through of a probability density function (PDF).

Fig. 3 shows the PDF. One can see that setting the threshold lower than the critical DP, the zero value, increases the probability of detection, but also produces an increase in the number of false alarms, due to the underlying noise of the real measurements. Thus, a threshold that is slightly greater than zero must be selected to avoid this problem and to design a

robust detection algorithm; 0.05 was the final threshold selected for use.

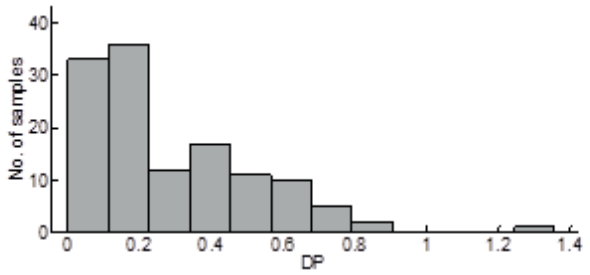

Figure 3: Results from designing the threshold over 127 disturbances.

Finally, the block diagram of the proposed technique is illustrated in Fig. 4. In this diagram, the signals are three-phase signals with no disturbance. In the residual generation block, the signals per phase are filtered and the residuals for each are obtained. Then, the residuals are treated using the CUSUM algorithm and the DP per phase is calculated. Finally, the diagnostic logic block makes the decision by using the established threshold and following the stopping rule: the start of a disturbance must be triggered (*T*) when the DP is across the threshold.

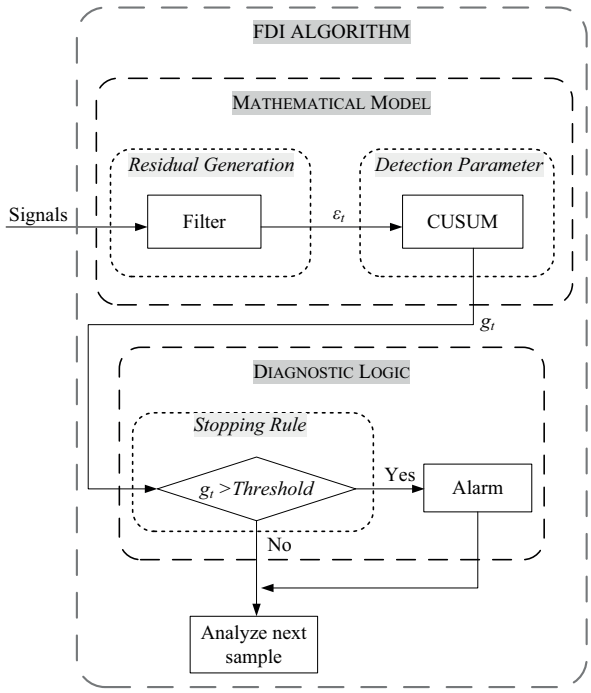

Figure 4: Block diagram of the proposed method for disturbance detection

This paper introduces further improvements in the algorithm and covers another critical issue in the online detection: the delayed detection. This issue is directly related to the ability of the selected algorithm to generate the detection signal alarm when a change occurs in real-time. An additional counter, called *N*, is used to reduce the effect of the analysis window and accurately calculate the start of the transition. The *N* parameter, introduced by Montgomery [32], estimates the first out of control instant of the process and indicates the number of consecutive times that the DP is non-zero after crossing *H*. Hence, the *N* parameter can be used to determine the time elapsed between the start of the transition (*S*) and the detection instant (*T*). Then, the non-stationary state of the process is triggered as a result of subtracting *N* from the initially set trigger point, *T*.

4 Experimental results

In order to validate the detector, other results from analysed measured signals are presented in this section. Considering that a design goal is to use the proposed technique alone for a wide range of PQ event parameters, the following cases are studied: dip, overvoltage, transient and interruption. All data used in this paper were obtained from measurements with the sampling rate f_s = 4800 Hz and 50 Hz power system frequency. Thus, each cycle contains 96 samples, or 20 ms. In this section, all of the signals' horizontal axes show the time in samples. The characteristics of the Butterworth used are 5th-order high pass, with a cut-off frequency of 3600 Hz.

Let us assume that the values of the DP that cross the threshold after a detected transition in the time of one cycle below are not considered to be transitions but effects of the previous transitions detected.

4.1 Dips

Fig. 5 shows a three-signal with a multi-stage dip (top graph) and the detection parameters with the same threshold (bottom graph).

From Fig. 5, one can see that there are three detection areas that correspond with the development between stages of the dip. The next figures, Figs. 6, 7 and 8, zoom into the detection areas. The DP per phase is individually shown in these figures, and the trigger instants *T* (vertical dashed line) and the calculated starting instant *S* (vertical solid line) are included in each one. Remember that *T* is the first instant when DP is across *H* (horizontal dashed line) and that *S* is the result of subtracting the counter *N* from *T*.

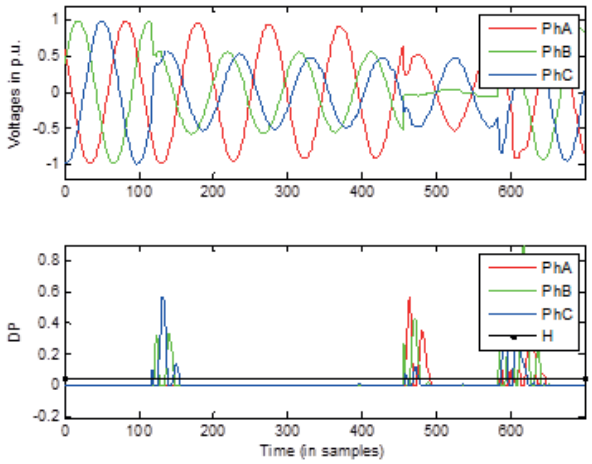

Figure 5: From top to bottom: input signal with multi-stage dip and detection parameters with the threshold

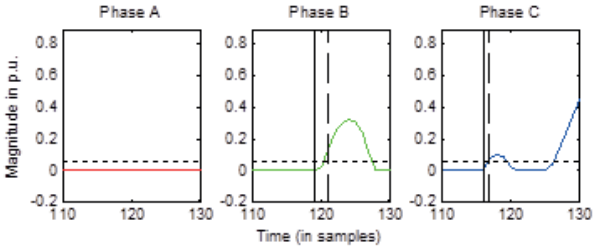

Figure 6: From left to right: zooms of the first detection area in phases A, B and C.

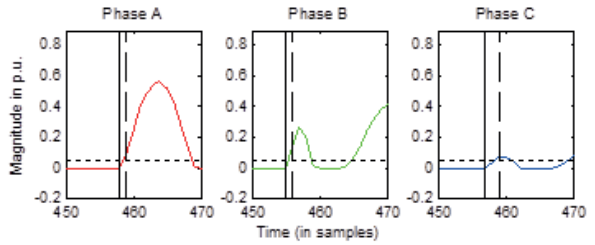

Figure 7: From left to right: zooms of the second detection area in phases A, B and C.

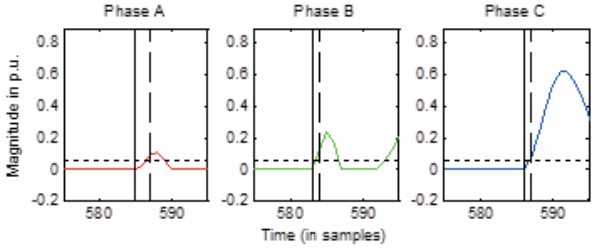

Figure 8: From left to right: zooms of the third detection area in phases A, B and C.

The detection instants calculated by the method are shown in samples in Table 1.

Table 1: Detection instants for multi-stage dip

Phase	First transition		Second transition		Third transition	
	T (sample)	S (sample)	T (sample)	S (sample)	T (sample)	S (sample)
A	-	-	459	458	587	585
B	121	119	456	455	584	583
C	117	116	459	457	587	586

For each detection transition area, the final trigger was set to the minimum value of the *S* parameter in the three phases. Hence, for the analysed dip, the final triggers were set at samples 116, 455 and 583, for the first, second and third areas, respectively. Figure 9 shows the original waveforms and the RMS voltage over a half-cycle rectangular window, with the triggers (vertical lines), showing the transitions.

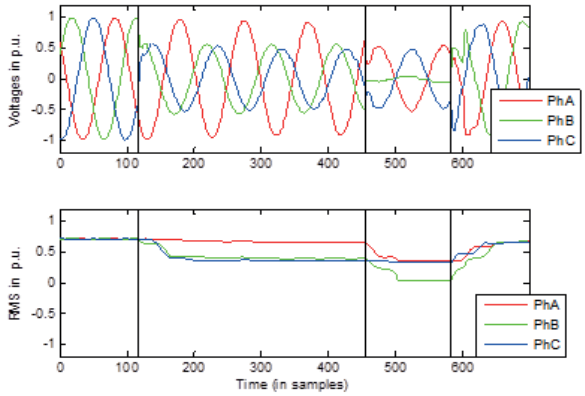

Figure 9: From top to bottom: input signal with triggers and RMS voltages with triggers.

4.2 Overvoltages

An example of a voltage dip due to single-phase fault with overvoltages in the non-faulted phases is shown in Fig. 10. As with in the prior case, there are three detection areas.

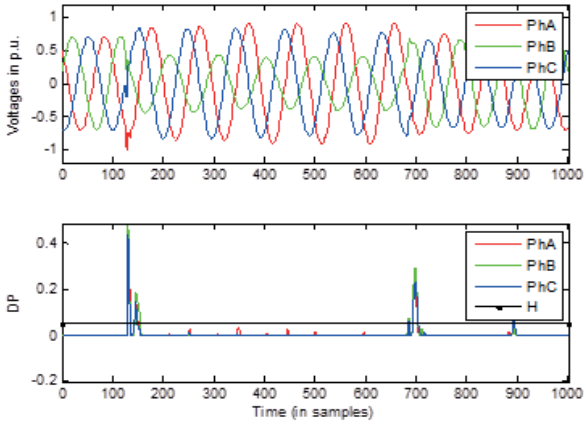

Figure 10: From top to bottom: input signal with overvoltage and detection parameters with the threshold.

The next figures, Figs 11, 12 and 13, zoom in on the detection areas.

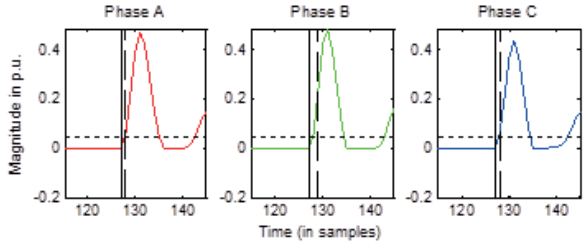

Figure 11: From left to right: zooms of the first detection area in phases A, B and C.

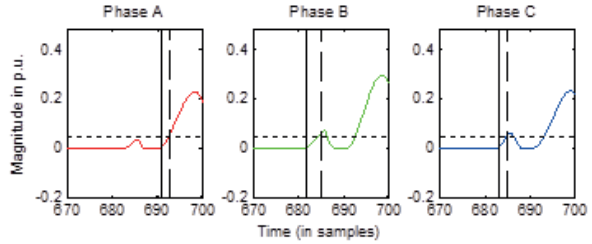

Figure 12: From left to right: zooms of the second detection area in phases A, B and C.

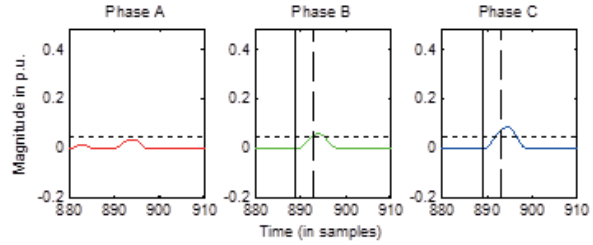

Figure 13: From left to right: zooms of the third detection area in phases A, B and C.

The detection instants, triggered instants *T* and the calculated starting instant *S* are shown in samples in Table 2.

Table 2: Detection instants for overvoltages.

Phase	First transition		Second transition		Third transition	
	T (sample)	S (sample)	T (sample)	S (sample)	T (sample)	S (sample)
A	128	127	693	691	-	-
B	129	127	685	682	893	889
C	128	127	685	683	893	889

The final triggers are set to the minimum value of the *S* parameter in the three phases per transition. Thus, the values of the triggers are set at samples 127, 682 and 889, for the first, second and third transition areas respectively. Fig. 14 shows the original waveforms and the RMS voltage over a half-cycle rectangular window with the triggers (vertical lines), showing the transitions.

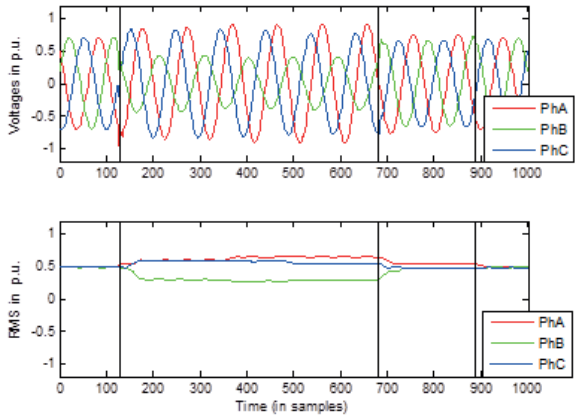

Figure 14: From top to bottom: input signal with triggers and RMS voltages with triggers.

4.3 Transients

In this case, the detection of a transient is presented. Fig. 15 shows the original waveform with the transient around sample number 500 and the DPs resulting from CUSUM. Fig. 16 shows a zoom of the original waveforms in the area of the transient. One can see that the three phases are affected by the disturbance. The DPs per phase in the transient area are individually shown and zoomed in Fig. 17. Also, the trigger instants *T* (vertical dashed line) and the calculated starting instant *S* (vertical solid line) are included in the graphs of Fig. 17. The trigger point (*T*) is sample 487 for phases A and B, and sample 490 for phase C. The starting instant (*S*) is sample 486 for phases A and B, and sample 488 for phase C. Thus, the final trigger was set to the sample 486. The final trigger is shown in Fig. 18 with the original waveforms and the RMS voltage over a half-cycle, rectangular window.

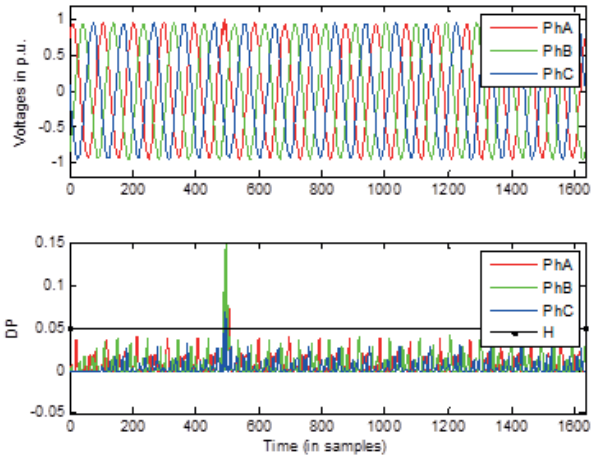

Figure 15: From top to bottom: input signal with transient and detection parameters with the threshold.

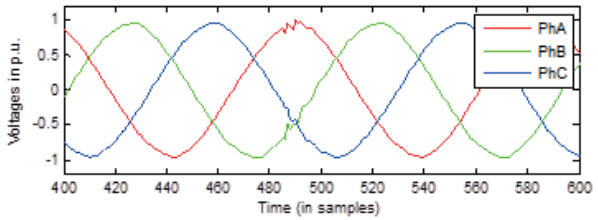

Figure 16: Zoom of the transient area.

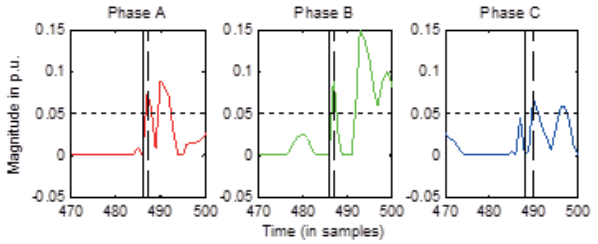

Figure 17: From left to right: zooms of the transitions for phases A, B and C.

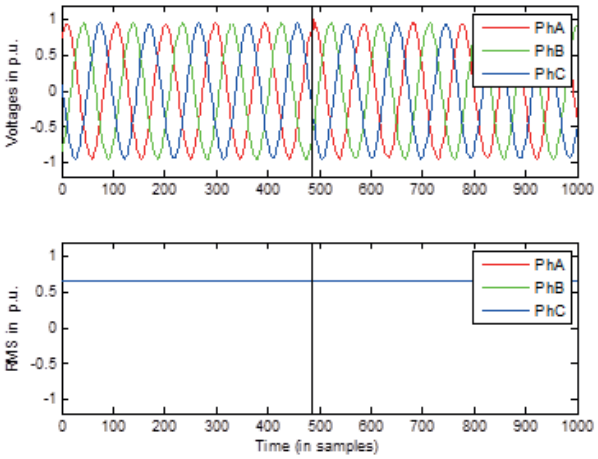

Figure 18: From top to bottom: input signal with the trigger and RMS voltages with the trigger.

4.4 Interruptions

Fig. 19 shows the original waveform of an interruption (top graph) and the calculated DPs per phase (bottom graph). Zooms of the detection parameters in the area of the interruption are individually shown in Fig. 20, including the trigger instants *T* (vertical dashed line) and the calculated starting instant *S* (vertical solid line). The trigger points (*T*) for phases A, B and C are sample 492, sample 489 and sample 484, respectively. The starting instants (*S*) for phases A, B and C are sample 491, sample 486 and sample 481, respectively. The final trigger is shown in Fig. 21, with the original waveforms and the RMS voltage over-half cycle rectangular window. The final trigger is set to the minimum value of the *S* parameter in the three phases, which occurs at sample 481.

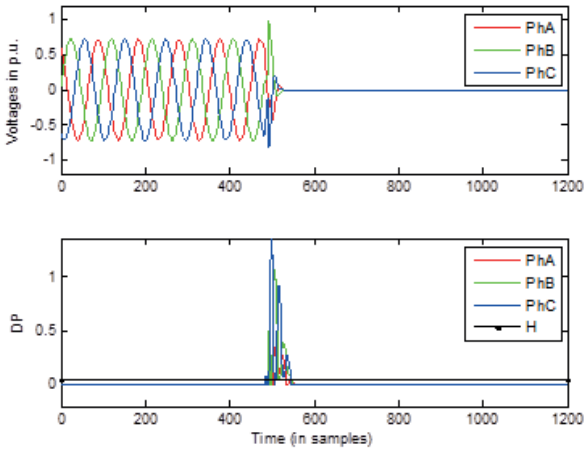

Figure 19: From top to bottom: input signal with the interruption and detection parameters with the threshold.

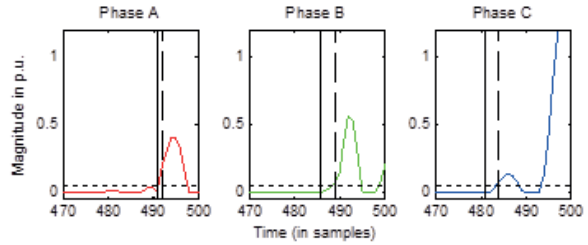

Figure 20: From left to right: zooms of the transitions in phases A, B and C.

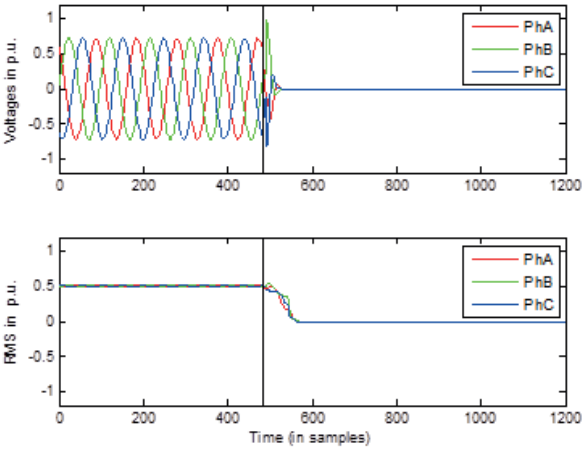

Figure 21: From top to bottom: input signal with the trigger and RMS voltages with the trigger.

5 Conclusions

The present study provides a useful technique for fast online detection of PQ events. The proposed method, based on the CUSUM algorithm as a statistical estimator, accurately detects the transition for three phases of different PQ events. Furthermore, the main advantages of the solution given in this paper are that the

CUSUM algorithm is extremely easy to implement and has very little computational burden, making it appropriate for an effective protection requirement. Another advantage of the CUSUM method is it performs sample-by-sample evaluation, making it suitable for early event detection. Moreover, the method overcomes the detection-delay problem inherent to the analysis windows of the conventional methods by including a counter that determines the time elapsed between the start of the transition and the detection instant. Additionally, a robust threshold setting for the detection index has been proposed, configured with high sensitivity and a low false-alarm rate. The CUSUM statistical estimator has been used to determinate the threshold. To this end, a probability density function of the detection parameter results has been made in order to apply CUSUM to a wide set of real measurement signals has been made. The implemented tests and experimental results show the effectiveness of this algorithm for detecting events and triggering with high precision the instant in which the three-phase signals start to deviate due to any disturbance. In summary, the proposed technique does not require much computational resolution and is very well chosen for implementation in protective relays. It is a robust detection algorithm that is capable of detecting PQ events in real-time.

6 Acknowledgements

This research is partially supported by FEDER-INNTERCONECTA project Total Integrated GRid Intelligent System (TIGRIS) ITC-20131002, under contract no. 12013095 and by FEDER-INNTERCONECTA project PV-On Time ITC-20131005, under contract no. 12013096. In addition, this work has been supported by the Spanish Ministry of Economy and Competitiveness under Project TEC2013-47316-C3-1-P.

7 References

1. Bassi AM. Evaluating the Use of an Integrated Approach to Support Energy and Climate Policy Formulation and Evaluation. Energies 2010;3:1604–21. doi:10.3390/en3091604.
2. Moreno-Muñoz A, De la Rosa JJG, López MA, Gil de Castro AR. Grid interconnection of renewable energy sources: Spanish legislation. Energy Sustain Dev 2010;14:104–9. doi:10.1016/j.esd.2010.03.003.
3. Elektrotechniker VD. Technical minimum requeriments for the connection to and parallel operation with the low-voltage distribution networks 2011.
4. Guerrero-Martínez M., Romero-Cadaval E, Minambres-Marcos V, Milanés-Montero MI. Supercapacitor Energy Storage System for Improving the Power flow in Photovoltaic Plants. Inf Midem-Journal Microelectron Electron Components Mater 2014;44(1):40–52.
5. IEC 61727. Photovoltaic (PV) systems – Characteristics of the utility interface. Int Electrothecnical Com 2004.
6. IEEE Std 1547. IEEE Standard for Interconnecting Distributed Resources with Electric Power Systems 2003:1–28.
7. V 0126-1-1. Automatic disconnection device between a generator and the public low-voltage grid. VDE 2013.
8. Fairley P. How rooftop solar can stabilize the grid [News]. IEEE Spectr 2015;52:11–3.
9. Katiraei F, Sun C, Enayati B. No Inverter Left Behind: Protection, Controls, and Testing for High Penetrations of PV Inverters on Distribution Systems. IEEE Power Energy Mag 2015;13:43–9.
10. Romero-Cadaval E, Minambres-Marcos VM, Moreno-Munoz A, Real-Calvo RJ, Gonzalez de la Rosa JJ, Sierra-Fernandez JM. Active functions implementation in smart inverters for distributed energy resources. 2013 Int. Conf. Compat. Power Electron., IEEE; 2013, p. 52–7.
11. Moreno-Garcia I-M, Moreno-Munoz A, Domingo-Perez F, Pallares-Lopez V, Real-Calvo R-J, Santiago-Chiquero I. Implementation of a Smart Grid Inverter through Embedded Systems. Electron Electr Eng 2013;19:3–6. doi:10.5755/j01.eee.19.3.1378.
12. Mahela OP, Shaik AG, Gupta N. A critical review of detection and classification of power quality events. Renew Sustain Energy Rev 2015;41:495–505. doi:10.1016/j.rser.2014.08.070.
13. De la Rosa JJG, Fernandez JMS, Ayora-Sedeno D, Aguera-Perez A, Palomares-Salas JC, Moreno-Munoz A. HOS-based virtual instrument for power quality assessment. 2011 7th Int. Conf. Compat. Power Electron., IEEE; 2011, p. 1–5.
14. De la Rosa JJG, Sierra-Fernandez JM, Aguera-Perez A, Sedeno DA, Palomares-Salas JC, Montero AJ, et al. HOS and CBR measurement system for PQ assessment. 11th Int. Conf. Electr. Power Qual. Util., IEEE; 2011, p. 1–6.
15]. De la Rosa JJG, Moreno-Munoz A, Palomares JC, Aguera A. Automatic classification of Power Quality disturbances via higher-order cumulants and self-organizing networks. 2010 IEEE Int. Symp. Ind. Electron., IEEE; 2010, p. 1579–84.
16. Gonzalez de la Rosa JJ, Aguera Perez A, Palomares Salas JC, Moreno-Munoz A. Amplitude-frequency classification of Power Quality transients using higher-order cumulants and Self-Organizing

Maps. 2010 IEEE Int. Conf. Comput. Intell. Meas. Syst. Appl., IEEE; 2010, p. 66–71.
17. De la Rosa JJG, Moreno-Munoz A, Gallego A, Piotrkowski R, Castro E. Spectral Kurtosis based system for transients' detection: Application to termite targeting. 2009 IEEE Sensors Appl. Symp., IEEE; 2009, p. 188–93.
18]. De la Rosa JJG, Moreno A, Puntonet CG. A Practical Approach To Higher-Order Statistics. An Application to Electrical Transients Characterization. 2007 IEEE Int. Symp. Intell. Signal Process., IEEE; 2007, p. 1–6.
19. Moreno-Muñoz A. Power Quality. Springer London; 2007. doi:10.1007/978-1-84628-772-5.
20. Bollen M, Gu I, Santoso S, Mcgranaghan M, Crossley P, Ribeiro M, et al. Bridging the gap between signal and power. IEEE Signal Process Mag 2009;26:12–31.
21. Gu IYH, Ernberg N, Styvaktakis E, Bollen MHJ. A Statistical-Based Sequential Method for Fast Online Detection of Fault-Induced Voltage Dips. IEEE Trans Power Deliv 2004;19:497–504.
22. De Apráiz M, Barros J, Diego RI. A real-time method for time–frequency detection of transient disturbances in voltage supply systems. Electr Power Syst Res 2014;108:103–12. doi:10.1016/j.epsr.2013.11.007.
23. Moschitta A, Carbone P, Muscas C. Performance Comparison of Advanced Techniques for Voltage Dip Detection. IEEE Trans Instrum Meas 2012;61:1494–502. doi:10.1109/TIM.2012.2183436.
24. Radil T, Ramos PM, Janeiro FM, Serra AC. PQ Monitoring System for Real-Time Detection and Classification of Disturbances in a Single-Phase Power System. IEEE Trans Instrum Meas 2008;57:1725–33. doi:10.1109/TIM.2008.925345.
25. Agüera-Pérez A, Carlos Palomares-Salas J, de la Rosa JJG, María Sierra-Fernández J, Ayora-Sedeño D, Moreno-Muñoz A. Characterization of electrical sags and swells using higher-order statistical estimators. Measurement 2011;44:1453–60. doi:10.1016/j.measurement.2011.05.014.
26.] IEEE 929. IEEE Recommended Practice for Utility Interface of Photovoltaic (PV) Systems 2000:i – .
27. Hwang I, Kim S, Kim Y, Seah CE. A Survey of Fault Detection, Isolation, and Reconfiguration Methods. IEEE Trans Control Syst Technol 2010;18:636–53.
28. Basseville M, Nikiforov IV. Detection of abrupt changes: theory and application. 1993.
29. Gustafsson F. Adaptive filtering and change detection. 2000.
30. Gudzius S, Markevicius LA, Morkvenas A. Characteristics of Fault Detection System for Smart Grid Distribution Network. Electron Electr Eng 2011;112:123–6.
31. Moreno-Garcia IM, Moreno-Munoz A, Domingo-Perez F, Lopez VP, Real-Calvo R, de la Rosa JJG. Smart Grid Inverter Interface: Statistical approach applied to event detection. 2012 IEEE Int. Work. Appl. Meas. Power Syst. Proc., IEEE; 2012, p. 1–6. doi:10.1109/AMPS.2012.6343987.
32. Montgomery DC. Introduction to Statistical Quality Control. 2008.
33. Kenny P. Better Business Decisions from Data: Statistical Analysis for Professional Success. Apress; 2014.
34. Montero-Hernandez OC, Enjeti PN. A Fast Detection Algorithm Suitable for Mitigation of Numerous Power Quality Disturbances. IEEE Trans Ind Appl 2005;41:1684–90. doi:10.1109/TIA.2005.857459.
35. Redfern MA, Al-Nasseri H. Protection of micro-grids dominated by distributed generation using solid state converters 2008:670–4.
36. Pires VF, Guerreiro M. A Current Differential Line Protection Using a Synchronous Reference Frame Approach 2008:198–203.
37. Kuen-Der Wu, Jou H-L. An orthogonal peak detector for multiphase sinusoidal signals. IEEE Trans Instrum Meas 2000;49:1216–23.
38. Mansor M, Rahim NA. Voltage sag detection - A survey. 2009 Int. Conf. Tech. Postgraduates, IEEE; 2009, p. 1–6.
39. Lee D-M, Habetler TG, Harley RG, Keister TL, Rostron JR. A Voltage Sag Supporter Utilizing a PWM-Switched Autotransformer. IEEE Trans Power Electron 2007;22:626–35. doi:10.1109/TPEL.2006.890004.
40. Teke A, Saribulut L, Tumay M. A Novel Reference Signal Generation Method for Power-Quality Improvement of Unified Power-Quality Conditioner. IEEE Trans Power Deliv 2011;26:2205–14.
41. Moreno-García I, Moreno-Muñoz A, Pallarés-López V, Real-Calvo R. Platform for Embedded Systems Design in the Smart Grid Framework. In: Sambath S, Zhu E, editors. Adv. Intell. Soft Comput., vol. 133, Berlin, Heidelberg: Springer Berlin Heidelberg; 2012, p. 593–600. doi:10.1007/978-3-642-27552-4.
42. Noori MR, Jamali S, Shahrtash SM. Security assessment for a cumulative sum-based fault detector in transmission lines. 2011 10th Int. Conf. Environ. Electr. Eng., IEEE; 2011, p. 1–5. doi:10.1109/EEEIC.2011.5874792.
43. Mohanty SR, Pradhan AK, Routray A. A Cumulative Sum-Based Fault Detector for Power System Relaying Application. IEEE Trans Power Deliv 2008;23:79–86.

44. Xingze He, Man-On Pun, Kuo C-CJ. Quickest detection of unknown power quality events for smart grids 2012:1–4.
45. Bollen MH, Gu I. Signal Processing of Power Quality Disturbances. Wiley; 2006.
46. Subasi A, Yilmaz AS, Tufan K. Detection of generated and measured transient power quality events using Teager Energy Operator. Energy Convers Manag 2011;52:1959–67.

Arrived: 06. 06. 2015
Accepted: 04. 09. 2015